PERGAMON

International Journal of Heat and Mass Transfer 42 (1999) 4549–4565

International Journal of HEAT and MASS TRANSFER

www.elsevier.com/locate/ijhmt

Homogeneous turbulence evolution in a stably stratified flow—III. Near time span at low inverse Froude number and distant time span at arbitrary Froude number

V.A. Babenko

A.V. Luikov Heat and Mass Transfer Institute, Belarussian Academy of Sciences, Minsk, Belarus

Received 17 February 1999

Abstract

This paper is the third and last part of work studying analytically and numerically the second-order turbulence model [B.A. Kolovandin, Modelling the dynamics of turbulent transport processes, in: Advances in Heat Transfer, vol. 21. Pergamon, 1991, pp. 185–234, and B.A. Kolovandin, V.U. Bondarchuk, C. Meola, G. De Felice, Modeling of the homogeneous turbulence dynamics of stably stratified media, Int. J. of Heat and Mass Transfer 36 (1993) 1953–1968] for homogeneous turbulence in stratified media. As in the two previous parts [V.A. Babenko, Homogeneous turbulence evolution in stably stratified flow—I. Internal gravity waves at low inverse Froude numbers, Int. J. of Heat and Mass Transfer 40 (1997) 1951–1961, and V.A. Babenko, Homogeneous turbulence evolution in stably stratified flow—II. Asymptotic regimes of large evolution time at low inverse Froude numbers. Int. J. of Heat and Mass Transfer 40 (1997) 1963–1976], the model is studied with asymptotic small parameter methods. In this part the inverse Froude number and the inverse evolution time are used for this purpose.

1. Introduction

The evolution of homogeneous turbulent flow in media with constant vertical gradients of density or temperature remains a keystone problem in the statistical fluid mechanics of turbulent heat and mass transfer [1]. This model problem of shearless turbulence can be considered as a realistic approach to describe turbulence evolution in atmospheric and oceanic streams, where there exists a stratification caused by the gravity force and the temperature or salinity drop. Among the application of this problem are ocean thermocline, the propagation of waste pollutants in the ocean and atmosphere, and wakes monitoring. Analytical reviews of the problem together with the data of experiments and numerical runs one can find in [1–8] as well as in previous parts of this paper [9,10].

In the first part [9], homogeneous turbulence in a density stratified medium was studied by parametric asymptotic expansion on an inverse Froude number Fr, represented by a ratio of inertia forces to buoyancy forces. This number is a perfect small parameter in the majority of practical important cases. Using the perturbation methods, non-linear internal gravity waves were analytically separated from the rest of turbulent motion and analytical expressions for the amplitudes and frequency of internal gravity waves were found. In the second part [10], some analytical solutions for the functions of the model were obtained in an asymptotic case of weak turbulence (i.e. in the final stage of turbulence decay) and the behavior of various turbulent characteristic scales was discussed. This paper considers two matters remaining unstudied in [9] and [10], namely approximate solution for near time span at

0017-9310/99/$ - see front matter
PII: S0017-9310(99)00054-X

Nomenclature

$E=\overline{u_i^2}/U^2$	dimensionless kinetic energy	$T_\rho=(\overline{\rho^2}U)/(\epsilon_\rho M)$	time scale of density field
$Fr=NM/U$	inverse Froude number	$\overline{u_i^2}$	doubled turbulence kinetic energy
M	cell size of a grid	U	flow velocity.
$N=(g\,\mathrm{d}\bar{\rho}/\bar{\rho}\,\mathrm{d}x_2)^{1/2}$	Brunt–Väisälä number		
$Q=(-\overline{u_2\rho})/(UM^{\mathrm{d}\bar{\rho}}/\mathrm{d}x_2)^2$	dimensionless turbulent transverse mass flux	*Greek symbols*	
$R_{22}=\overline{u_2^2}/U^2$	vertical component of velocity pulsation tensor	ϵ_u	dissipation rate of velocity fluctuations
$Re=UM/\nu$	Reynolds number $\tilde{\tau}=\sqrt{\epsilon}\tau=N\tau*$	ϵ_ρ	dissipation rate of density fluctuations
$R_\lambda=(5ET_u\,Re)^{1/2}$	turbulent Reynolds number	$\Theta=\overline{\rho^2}/(M^{\mathrm{d}\bar{\rho}}/\mathrm{d}x_2)^2$	squared density fluctuation
$t=Fr\;T_\rho$	fast and slow time variables	σ	molecular Prandtl number
$T_u=(\overline{u_i^2}U)/(\epsilon_u M)$	time scale of velocity field	τ^*	dimensional time
		$\tau=\tau^*U/M$	dimensionless time.

$Fr\ll 1$ and analysis for far time span at an arbitrary Froude number.

2. Governing equations

In the Boussinesq approximation both the cases of temperature and density stratification look identical. To be more definite we shall discuss density stratification further.

The system of ordinary differential equations from [6] for modeling the stratified turbulence can be written in dimensionless form as (see [9])

$$\frac{\mathrm{d}R_{22}}{\mathrm{d}\tau}=-\frac{2}{3}\frac{E}{T_u}\left[d+\frac{9}{2}(1-d)\right]\left(3\frac{R_{22}}{E}-1\right)-\frac{2}{3}\frac{E}{T_u}-\frac{8}{5}Q\,Fr^2,$$

$$\frac{\mathrm{d}E}{\mathrm{d}\tau}=-2\left[1+Q\frac{T_u}{E}Fr^2\right]\frac{E}{T_u},$$

$$\frac{\mathrm{d}T_u}{\mathrm{d}\tau}=(F_u^{**}-2)-2Fr^2\frac{QT_u}{E}\times\left[1-\left(\frac{2\sigma}{1+\sigma}\right)\left(\sigma_\infty+\frac{3}{5}\right)\frac{d}{R_\infty}\frac{T_u}{T_\rho}\right],$$

$$\frac{\mathrm{d}Q}{\mathrm{d}\tau}=-\left[\frac{2}{3}-\frac{1}{Fr^2}\frac{R_{22}}{\Theta}-d\left(\frac{R_{22}}{E}-\frac{1}{3}\right)\right]Fr^2\Theta-(1-d)\times\left(\frac{1}{3}+10\frac{R_{22}T_u}{ET_\rho}\right)\frac{Q}{T_u}-2\left(\sigma_\infty+\frac{3}{5}\right)\frac{d}{R_\infty}\frac{T_u}{T_\rho}\frac{Q}{T_u},$$

$$\frac{\mathrm{d}\Theta}{\mathrm{d}\tau}=-2\left[1-Q\frac{T_\rho}{\Theta}\right]\frac{\Theta}{T_\rho},$$

$$\frac{\mathrm{d}T_\rho}{\mathrm{d}\tau}=(F_{\rho 2}^{**}-2)+F_{\rho 1}^{**}\frac{T_\rho}{T_u}-d\frac{4}{3}\left(1-\frac{3}{5R_\infty}\right),\qquad(1)$$

where the asymptotic values of the turbulent Prandtl number, σ_∞, and the time scale ratio R_∞ at infinity time in a passive scalar case ($Fr=0$) are taken from [11].

$$\sigma_\infty=\frac{3(1-\sigma)}{10\sigma}\left[1-\left(\frac{2\sigma}{1+\sigma}\right)^{3/2}\right]^{-1},\qquad(2)$$

$$R_\infty=\frac{1}{5\sigma}\left[1-\left(\frac{2\sigma}{1+\sigma}\right)^{3/2}+\sigma^{3/2}\right]\times\left[1-2\left(\frac{2\sigma}{1+\sigma}\right)^{1/2}+\sigma^{1/2}\right]^{-1}.\qquad(3)$$

In theory [12] empiric functions F_u^{**}, $F_{\rho 1}^{**}$ and $F_{\rho 2}^{**}$ were used to model an interaction of vortexes with different

scales in velocity and scalar fields. They depend exclusive upon the turbulence Reynolds number R_λ through the function $\mathrm{d}(R_\lambda^2) = 1 - 2/(1+\sqrt{1+\delta_u/R_\lambda^2})$, where $\delta_u = 2800$ (see [12])

$$F_u^{**} = \tfrac{11}{3} - \tfrac{13}{15}d, \quad F_{\rho 1}^{**} = \tfrac{5}{3}(1-d), \quad F_{\rho 2}^{**} = 2 + \tfrac{4}{3}d.$$

The function $\mathrm{d}(R_\lambda^2)$ represents turbulence inertia effects in equations and separates the regimes of strong ($d \to 0$ at $R_\lambda \gg 1$) and weak ($d \to 1$ at $R_\lambda \ll 1$) turbulence.

3. Near time span

In this section for a small stratification case (when the inverse Froude number Fr is small) we shall consider a near time span extended approximately over three first periods of internal waves. Near time span is characterized by the large initial turbulence Reynolds number R_λ and the small value of wave-averaged vertical mass flux.

For the analysis of near time span we shall slightly alter a set of main variables, as compared with those in [9]. It allows one to group the terms of Eqs. (1) alternatively in accordance with their magnitudes. Namely, we change the definition of dimensionless mass flux q. The new variable is defined as $q_1 = q/e$, where $e \equiv Fr$ is a small parameter. Other main variables remain unchanged

$$q_1 = eT_\rho Q/E, \quad \vartheta = \epsilon\Theta/E, \quad K = R_{22}/E,$$

$$R = T_u/T_\rho, \quad t = \epsilon T_\rho, \quad \tilde{\tau} = e\tau. \tag{4}$$

In (4) the variable q_1 represents the flux Richardson number, ϑ is the ratio of the potential energy of density fluctuations $\epsilon\Theta$ to the turbulence kinetic energy E, K is the fraction of turbulence kinetic energy (TKE) stored in vertical velocity fluctuations, R the time scale ratio, t the density field time scale multiplied by $\epsilon = e^2$. In terms of these new variables the system of Eqs. (1) can be rewritten as

$$t\frac{\mathrm{d}K}{\mathrm{d}\tilde{\tau}} = e\frac{-7d'(K-1/3)}{R} + 2\epsilon q_1(K-4/5),$$

$$t\frac{\mathrm{d}R}{\mathrm{d}\tilde{\tau}} = \frac{4}{5}ed(1-R/R_\infty) - 2\epsilon q_1(1-\alpha_2 R)R,$$

$$t\frac{\mathrm{d}\vartheta}{\mathrm{d}\tilde{\tau}} = 2e\left(\frac{1}{R}-1\right)\vartheta + 2\epsilon q_1(1+\vartheta),$$

$$\epsilon t\frac{\mathrm{d}q_1}{\mathrm{d}\tilde{\tau}} = t^2A_1 + 2\epsilon^2 q_1^2 + \epsilon e q_1\left[\frac{1}{R}\left(2-\frac{d'}{3}\right) - 10d'K - \alpha_1 + p\right],$$

$$t\frac{\mathrm{d}E}{\mathrm{d}\tilde{\tau}} = -e\frac{2E}{R} - 2\epsilon q_1 E,$$

$$\frac{\mathrm{d}T}{\mathrm{d}\tilde{\tau}} = ep \tag{5}$$

where $\alpha_1 = 2d(\sigma_\infty + 3/5)/R_\infty$, $\alpha_2 = \alpha_1\sigma/(1+\sigma)$ are the functions dependent on $\mathrm{d}(R_\lambda^2)$ and σ, $p = 4d/5R_\infty + 5d'/3R$, $d' = 1-d$ and A_1 is the function $A_1(K, d, \vartheta) = K + \vartheta[d(K-1/3)-2/3]$.

Further, we shall need two auxiliary differential equations, one for the function A_1 and another for $\mathrm{d}(R_\lambda^2)$. They can be easily obtained from their definitions and system (5)

$$t\frac{\mathrm{d}A_1}{\mathrm{d}\tilde{\tau}} = 2(ec_1 + \epsilon c_2 q_1), \tag{6}$$

$$t\frac{\mathrm{d}(d)}{\mathrm{d}\tilde{\tau}} = -p_1\left[e\frac{\frac{1}{3}+\frac{13}{15}d}{R} - 2\epsilon q_1(2-\alpha_2 R)\right], \tag{7}$$

where

$$c_1 = -\frac{7}{2}(1+\vartheta d)\,d'\left(K-\frac{1}{3}\right)\frac{1}{R} + \vartheta\left[d\left(K-\frac{1}{3}\right)-\frac{2}{3}\right] \times \left(\frac{1}{R}-1\right) + \vartheta\left(K-\frac{1}{3}\right)\frac{p_1}{2}(F_u^{**}-4)\frac{1}{R},$$

$$c_2 = (1+\vartheta d)\left(K-\frac{4}{5}\right) + \left[d\left(K-\frac{1}{3}\right)-\frac{2}{3}\right](1+\vartheta) + \vartheta\left(K-\frac{1}{3}\right)p_1(2-\alpha_2 R),$$

and p_1 is a logarithmic derivative of d with respect to R_λ^2: $p_1 = [\mathrm{d}(d)/\mathrm{d}(R_\lambda^2)]R_\lambda^2 = (1/(1+\delta_u/R_\lambda^2)^{1/2}-1) \times (1+(1+\delta_u/R_\lambda^2)^{1/2})^{-1} = -dd'/(1+d)$.

At large t the problem (5) is singular in a sense of asymptotic expansions. It is caused by the fact that the fourth equation of system (5) degenerates into the algebraic form: $t^2A_1 = 0$ at $t \gg 1$. Alternatively, using a small perturbation approach, we can see that the fourth equation in (5) degenerates into an algebraic form $t^2A_1 = 0$ at $e \to 0$.

To avoid a singularity in asymptotic expansions we shall use a two-scale decomposition [13,14] and introduce the pair of time variables, t and $\tilde{\tau}$. The outer variable t is shrunk with regard to the variable $\tilde{\tau}$ and so is preferable at large $\tilde{\tau}$. At small t (that is in initial

time span), the variable $\tilde{\tau}$ can be thought of as an inner (or stretched) one because $\tilde{\tau} \sim t/e$.

Considering the functions in (5)–(7) as being dependent on two time variables τ and t we shall expand them on exponents of the small parameter e, as it was done earlier in [9]

$$f = \hat{f}(t) + \epsilon\tilde{f}(t,\tilde{\tau}) + \cdots,$$
$$q_1 = \hat{q}_1(t) + e\tilde{q}_1(t,\tilde{\tau}) + \cdots, \tag{8}$$

where f is one of the functions from systems (5)–(7) besides q_1. In (8) the first exponent of e is absent for all the variables except for q_1, thus reflecting the fact, that these functions depend on the inner variable $\tilde{\tau}$ starting from the second-order terms. It can be seen from (5), where at $e = 0$ these functions are constants.

Substituting (8) into systems (5)–(7), with the derivatives being decomposed according to formula $(\mathrm{d}/\mathrm{d}\tilde{\tau}) = (\partial/\partial\tilde{\tau}) + ep(\partial/\partial t)$, and combining the terms with identical exponents of e we get two sets of equations

$$t\hat{p}\frac{\mathrm{d}\hat{K}}{\mathrm{d}t} = -7\hat{d}'(\hat{K} - 1/3)\hat{R}^{-1},$$

$$t\hat{p}\frac{\mathrm{d}\hat{R}}{\mathrm{d}t} = \frac{4}{5}\hat{d}(1 - \hat{R}/R_\infty),$$

$$t\hat{p}\frac{\mathrm{d}\hat{\vartheta}}{\mathrm{d}t} = 2(\hat{R}^{-1} - 1)\hat{\vartheta},$$

$$t^2\hat{A}_1 = 0,$$

$$t\hat{p}\frac{\mathrm{d}\hat{d}}{\mathrm{d}t} = -\hat{p}_1\hat{R}^{-1}\left(\frac{1}{3} + \frac{13}{15}\hat{d}\right),$$

$$t\hat{p}\frac{\mathrm{d}\hat{E}}{\mathrm{d}t} = -2\hat{E}\hat{R}^{-1}, \tag{9}$$

$$t\frac{\partial\tilde{K}}{\partial\tilde{\tau}} = 2\hat{q}_1(\hat{K} - 4/5),$$

$$t\frac{\partial\tilde{R}}{\partial\tilde{\tau}} = -2\hat{q}_1(1 - \hat{\alpha}_2\hat{R})\hat{R},$$

$$t\frac{\partial\tilde{\vartheta}}{\partial\tilde{\tau}} = 2\hat{q}_1(1 + \hat{\vartheta}),$$

$$\frac{\partial\hat{q}_1}{\partial\tilde{\tau}} = t\tilde{A}_1,$$

$$t\frac{\partial\tilde{d}}{\partial\tilde{\tau}} = -2\hat{p}_1\hat{q}_1(2 - \hat{\alpha}_2\hat{R}),$$

$$t\frac{\partial\tilde{E}}{\partial\tilde{\tau}} = -2\hat{q}_1\hat{E}, \tag{10}$$

and one more equation deriving the dependence of the first term in expansion for turbulent mass flux on t

$$t\hat{p}\frac{\partial\hat{q}_1}{\partial t} + t\frac{\partial\tilde{q}_1}{\partial\tilde{\tau}} = \hat{q}_1\hat{c}_3, \tag{11}$$

where $\hat{c}_3 = \hat{R}^{-1}(2 - \hat{d}'/3) - 10\hat{d}'\hat{K} - \hat{\alpha}_1 + \hat{p}$, all the functions with 'hats' are calculated with the first terms of decompositions (8) and $\tilde{A}_1$ is the second term in decomposition for A_1: $A_1 = \hat{A}_1(t) + \epsilon\tilde{A}(t,\tilde{\tau}) + \cdots$.

Splitting Eq. (6) on the exponents of e results in

$$t\hat{p}\frac{\mathrm{d}\hat{A}_1}{\mathrm{d}t} = 2\hat{c}_1, \quad t\frac{\partial\tilde{A}_1}{\partial\tilde{\tau}} = 2\hat{c}_2\hat{q}_1.$$

Differentiating partially on $\tilde{\tau}$ the fourth line of (10) and substituting the last expression leads to a wave equation for $\hat{q}_1$

$$\frac{\partial^2\hat{q}_1}{\partial\tilde{\tau}^2} + \omega^2\hat{q}_1 = 0 \tag{12}$$

where $\omega^2 = -2\hat{c}_2(t)$. Writing this expression for the frequency in more detail, we have

$$-\frac{\omega^2}{2} = (1 + \hat{\vartheta}\hat{d})(\hat{K} - \tfrac{4}{5}) + [\hat{d}(\hat{K} - \tfrac{1}{3}) - \tfrac{2}{3}](1 + \hat{\vartheta}) + \hat{\vartheta}(\hat{K} - 1/3)p_1(2 - \alpha_2\hat{R}). \tag{13}$$

The form of this relation for the frequency coincides with that in [9] with the only difference that here the oscillations take place in the first term of decomposition but not in the second one as in [9]. The first term $\hat{q}$ in [9] was a non-zero wave-averaged mass flux. In the present analysis it is absent.

The third and the fourth lines of system (9) contradict each other since the function $\hat{\vartheta}$ can be found differently from them. At very small t, $t \ll 1$, the fourth line of (9), $\hat{t}^2\hat{A}_1 = 0$, should be omitted, since the value of $\hat{A}_1$ becomes indefinite in this case. At $t \gtrsim 1$, alternatively, the third line of (9) should be dropped, because it was obtained as the equation of lower order in decomposition.

In [9] the expression like (11) was used for the determination of $\tilde{q}$ at known $\hat{q}(t)$. Here it is served to find out the dependence $\hat{q}_1(t)$. Doing so, the derivative $\partial\tilde{q}_1/\partial\tilde{\tau}$ in (11) should be neglected in order to close the analysis and fir the number of unknown functions to the number of equations in (9) and (10). After this, the variables in (11) and (12) are separated with the substitution $\hat{q}_1 = \hat{q}_1'(t)\hat{q}_1''(\tilde{\tau})$ and we get the ordinary

differential equations for the amplitude $\hat{q}_1'(t)$ and phase $\hat{q}_1''(\tilde{\tau})$ of mass flux oscillation

$$t\hat{p}\frac{\mathrm{d}\hat{q}_1'}{\mathrm{d}t}=\hat{q}_1'\hat{c}_3,\quad \frac{\mathrm{d}^2\hat{q}_1''}{\mathrm{d}\tilde{\tau}^2}+\omega^2\hat{q}_1''=0 \tag{14}$$

Note, that Eqs. (9) and (14) could also be deduced as the special case of analysis [9] if we set $\hat{q}=0$. In this case the second term in decomposition for q becomes the leading one and it is obeyed in relations (14). Thus, the considered approach of near time span is simply a partial case of more common analysis from [9]. Below we shall make comparisons with [9].

The equations for $\hat{K}$, ϑ, and $\hat{E}$ in (9) can be solved separately after solving the pair of equations for $\hat{d}$ and $\hat{R}$. The variable $\hat{d}$ can be considered as a new independent variable. In this case the variables in the equation for $\hat{R}$ are separated

$$\frac{\mathrm{d}\hat{R}}{\hat{R}(1-\hat{R}/R_\infty)}=\frac{4}{5}\frac{(1+\hat{d})\,\mathrm{d}(\hat{d})}{(1-\hat{d})(\frac{1}{3}+\frac{13}{15}\hat{d})}. \tag{15}$$

Integrating in (15) gives

$$\frac{1}{\hat{R}}-\frac{1}{R_\infty}=\left(\frac{1}{R_0}-\frac{1}{R_\infty}\right)\times\left[\left(\frac{5+13d_0}{5+13\hat{d}}\right)^{4/3}\frac{1-\hat{d}}{1-d_0}\right]^{4/3}. \tag{16}$$

Similarly, the solution of the first and sixth equations in (9) can be written in the forms $\hat{K}(\hat{d})$ and $\hat{E}(\hat{d})$.

$$\hat{K}=\frac{1}{3}+\left(K_0-\frac{1}{3}\right)\left(\frac{d}{d_0}\right)^{-21}\left(\frac{5+13\hat{d}}{5+13d_0}\right)^{168/13}, \tag{17}$$

$$\hat{E}=E_0\left(\frac{1-\hat{d}}{1-d_0}\right)^{10/3}\left(\frac{d_0}{\hat{d}}\right)^{6}\left(\frac{5+13\hat{d}}{5+13d_0}\right)^{8/3}. \tag{18}$$

It is not difficult to express in quadratures the dependencies on $\hat{d}$ of the other functions with 'hats' in (9). For $\vartheta(\hat{d})$ we have

$$\hat{\vartheta}=\vartheta_0\ \exp\int_{d_0}^{\hat{d}}\frac{2(1+\hat{d})(1-\hat{R})}{\hat{d}(\frac{1}{3}+\frac{13}{15}\hat{d})(1-\hat{d})}\mathrm{d}(\hat{d}), \tag{19}$$

where $\hat{R}(\hat{d})$ is calculated according to (16). It is more convenient to take this integral numerically, as well as in the corresponding relation for $\hat{d}(t)$ arising at integrating in the fifth line of (9).

$$\int_{d_0}^{\hat{d}}\frac{(1+\hat{d})\hat{p}\hat{R}}{\hat{d}(\frac{1}{3}+\frac{13}{15}\hat{d})(1-\hat{d})}\mathrm{d}(\hat{d})=\int_{t_0}^{t}\frac{\mathrm{d}t}{t}. \tag{20}$$

It follows from (16)–(19), that in near time span the variance of the functions is dictated by the variance of the parameter $\hat{d}$ or the turbulent Reynolds number R_λ. The functions $\hat{K}(\hat{d})$ and $\hat{E}(\hat{d})$ do not depend on the molecular Prandtl number. The same refers to the universal dependence of the ratio $(\hat{R}^{-1}-R_\infty^{-1})/(R_0^{-1}R_\infty^{-1})=f(\hat{d})$. As the ratio $(\hat{d}/\hat{d}_0)$ grows, the relation (17) describes a very fast tendency of $\hat{K}$ to the isotropic value 1/3. At small $\hat{d}$ the term in square brackets in (16) decreases with increasing $\hat{d}$. Hence, whether the function $\hat{R}$ should increase or decrease, depends on the sign of the difference $(R_0^{-1}-R_\infty^{-1})$. If this difference is negative, as in the case of water, $\hat{R}$ decreases. In the case of air with this difference being positive, the value of $\hat{R}$ increases. The rate of the variance of $\hat{R}$ is slowed down with time. It is determined by decreasing the first factor in square brackets in (16).

A more full analysis can be carried out taking the assumption $d\ll 1$. In this case differential equations (9) and (14) can be simplified to:

$$\frac{5}{3}t\frac{d(\hat{K}-1/3)}{\mathrm{d}t}=-7\left(\hat{K}-\frac{1}{3}\right),\quad \frac{5}{3}t\frac{\mathrm{d}\hat{R}}{\mathrm{d}t}=\frac{4}{5}\hat{d}\left(1-\frac{\hat{R}}{R_\infty}\right),$$

$$\frac{5}{3}t\frac{\mathrm{d}\hat{\vartheta}}{\mathrm{d}t}=2(1-\hat{R})\hat{\vartheta},\quad \frac{5}{3}t\frac{\mathrm{d}\hat{d}}{\mathrm{d}t}=\frac{1}{3}\hat{d},$$

$$\frac{5}{3}t\frac{\mathrm{d}\hat{E}}{\mathrm{d}t}=-2\hat{E},\quad \frac{5}{3}t\frac{\mathrm{d}\hat{q}_1'}{\mathrm{d}t}=10\hat{q}_1'\left(\frac{1}{3}-\hat{K}\hat{R}\right). \tag{21}$$

The solutions of (21) for $\hat{K}$, $\hat{R}$, $\hat{d}$, and $\hat{E}$ are the following:

$$(\hat{K}-1/3)/(K_0-1/3)=(\hat{d}/d_0)^{-21},$$

$$\left(\frac{1}{R}-\frac{1}{R_\infty}\right)/\left(\frac{1}{R_0}-\frac{1}{R_\infty}\right)=\exp\left(-\frac{12}{5}(\hat{d}-d_0)\right),$$

$$\hat{E}/E_0=(\hat{d}/d_0)^{-6},$$

$$\hat{d}/d_0=y^{1/5}, \tag{22}$$

where $y=t/t_0$. Because of the function $\hat{d}$ and d_0 being small, the difference $\hat{d}-d_0$ in the expression for $\hat{R}$ (22) is also small, and the equation for ϑ in (21) can be solved for the 'frozen' value of $\hat{R}$. This assumptions results in the power solution

$$\hat{\vartheta}=\vartheta_0 y^{6/5(1-\hat{R})}. \tag{23}$$

In the case $\hat{R}<1$, which is characteristic of gases with a molecular Prandtl number $\sigma<1$, expression (23) describes a near power decrease of ϑ and, oppositely, a

near power growth in media with $\sigma > 1$. Expression (23) is appropriate only at low t when $t^2 \ll 1$. With growing t it should be replaced by the algebraic relation following from the fourth line of (9):

$$\hat{\vartheta} = \frac{\hat{K}}{2/3 - \hat{d}(\hat{K} - 1/3)}. \tag{24}$$

Finally, let us simplify the equation for amplitude $\hat{q}_1'$ at $\hat{d} \ll 1$. Taking into account a fast tendency of $\hat{K}$ to 1/3 and a 'frozen' value of $\hat{R}$, Eq. (14) can be presented in a form of near power law

$$\frac{t}{\hat{q}_1'} \frac{\mathrm{d}\hat{q}_1'}{\mathrm{d}t} \simeq 2(1 - \hat{R}). \tag{25}$$

The expression for the frequency of oscillations (13) at small $\hat{d}$ can be simplified up to

$$\omega^2 = -2[(\hat{K} - 4/5) - \tfrac{2}{3}(1 + \hat{\vartheta})] = 4(\tfrac{11}{15} - \hat{K}).$$

Substituting the solution for the first term of vertical mass flux $\hat{q}_1(t, \tau) = \hat{q}_1'(t) \sin(\omega\hat{\tau} + \phi)$ into the equations of system (10) we can obtain a number of simple relationships between phases and amplitudes of oscillations in various functions of the model. Here they are omitted for brevity because they completely coincided with those deduced earlier for a distant region (formulae (21)–(26) from [9]) if replacing $\tilde{q}'$ with $\hat{q}_1'$. Similar expressions will be repeated in the next section.

For the validity check of the dependencies obtained above they were compared with the numerical solution of system (1) with Gear's method. An initial data set was taken from Ref. [6] for $\sigma = 800$ and $Fr = 3.67 \times 10^{-2}$: $R_{22_0} = 3.47 \times 10^{-4}$, $E_0 = 1.33 \times 10^{-3}$, $T_{\rho_0} = 38.4$, $T_{u_0} = 43.3$, $Q_0 = 3.31 \times 10^{-3}$, $\Theta_0 = 0.153$. This data set corresponds to one of the experimental points from Ref. [2].

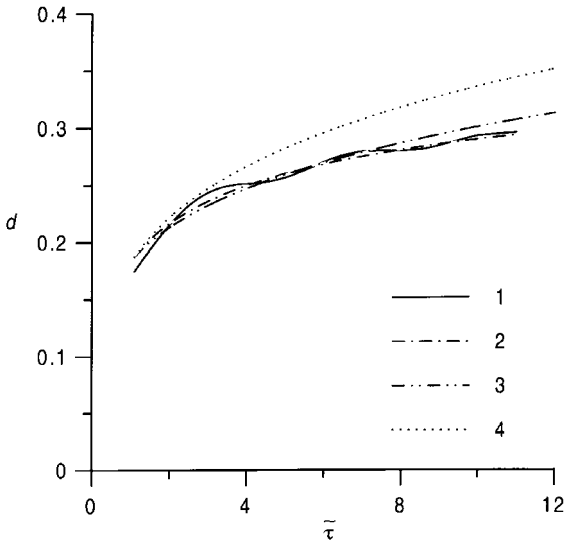

Fig. 1. Plot of various dependencies for the functions $d(\tilde{\tau})$ and $\hat{d}(\tilde{\tau})$: 1. d in numerical computation by system (1); 2. $\hat{d}$ according to computation in [9]; 3. $\hat{d}$ according to formula (2); 4. $\hat{d}$ according to (22).

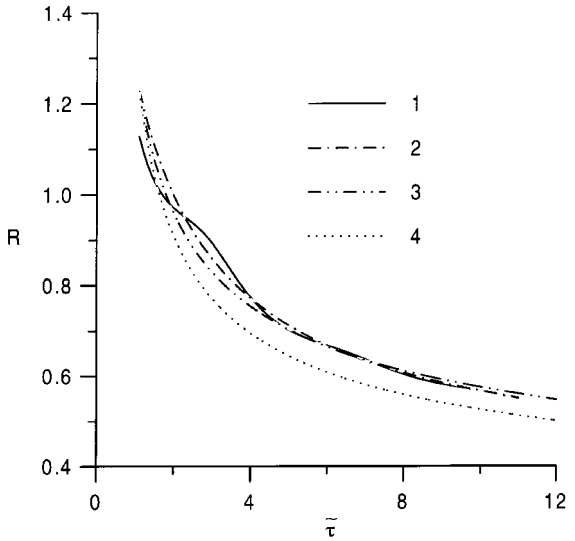

Fig. 2. Plot of various dependencies for the functions $R(\tilde{\tau})$ and $\hat{R}(\tilde{\tau})$: 1. R in numerical computation by system (1); 2. $\hat{R}$ according to computation in [9]; 3. $\hat{R}$ according to formula (16); 4. $\hat{R}$ according to (22).

Fig. 1 shows the comparison of two analytical expressions for the function $\hat{d}(\tilde{\tau})$ in a near time span, (20) and (22), with the numerical solution of system (1). In the numerical run the function $\hat{d}(\tilde{\tau})$ grows a little more slowly, than in expression (22), which sets the law of 'one-fifth'. The more general expression (20) corresponds better to the numerical solution. Initial conditions for the functions with 'hats' were found as it was described in [9].

For the time scale ratio $R(\tilde{\tau})$ the comparison of a full numerical solution, smoothed solution (Eqs. (9) and (15) from [9]), and two analytical expressions [one of general form in the near area approach, (16), and another at $d \ll 1$, (22)] is represented in Fig. 2. With a growth of time an agreement between the numerical and the analytical solution is worsened.

Fig. 3 plots the same comparison for the kinetic energy of turbulence $E(\tilde{\tau})$. As in the two previous figures, the solution of (18) is very close to the full numerical solution, while analytical power solution (22), which is characteristic of isotropic medium, gives the lower values of kinetic energy.

Analytical solutions for $\hat{K}(\hat{d})$ at small $\hat{d}$, (22) and in a more common case, (17), correspond worse to the

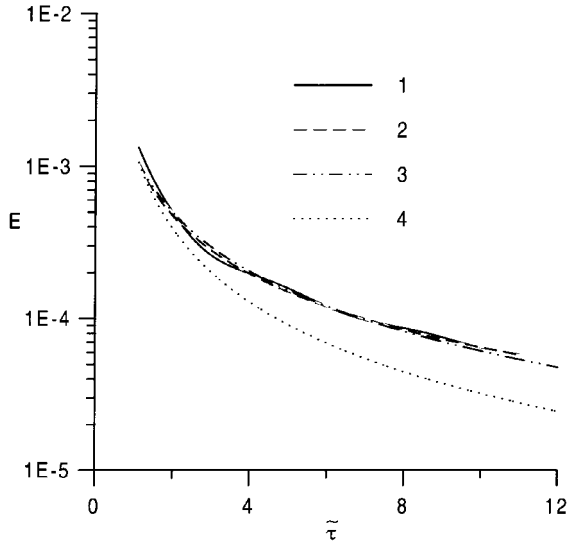

Fig. 3. Plot of various dependencies for the functions $E(\tilde{\tau})$ and $\hat{E}(\tilde{\tau})$: 1. E in numerical computation by system (1); 2. $\hat{E}$ according to computation in [9]; 3. $\hat{E}$ according to formula (18); 4. $\hat{E}$ according to (22).

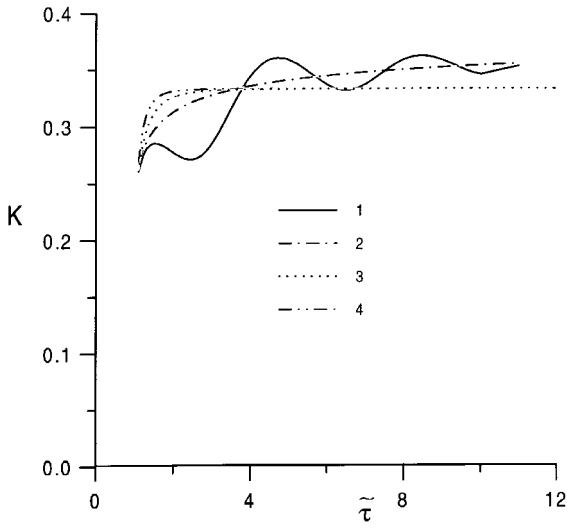

Fig. 4. Plot of various dependencies for the functions $K(\tilde{\tau})$ and $\hat{K}(\tilde{\tau})$: 1. K in numerical computation by system (1); 2. $\hat{K}$ according to computation in [9]; 3. $\hat{K}$ according to formula (17); 4. $\hat{K}$ according to (22).

numerical computation because their internal property has the presence of asymptotics $\hat{K}=1/3$ (Fig. 4). Clearly formed asymptotic regime $\hat{K}=1/3$ is observed in numerical runs only at very small ϵ. With increasing ϵ the slope of a weakly inclined part of the plot $\hat{K}(\tilde{\tau})$ grows and this intermediate asymptotic disappears. As in the previous figures, the solution of the 'smoothed' differential system from [9] describes the wave averaged behavior of the numerical solution very well.

The time interval, during which the power solution for ϑ, (23), accords with the numerical one (Fig. 5), appears very small. A more accurate solution, (19), is closer to the numerical data, however, it still remains unsatisfactory. Since in the initial data the condition $t\gg1$ took place, a more successful approach for $\hat{K}(\hat{d})$, than (23) and (19), can be expressed in accordance with formula (24).

In the equations of system (9) and (10), the function $\hat{q}_1$ is a kind of passive admixture. It can be determined after solving system (9). Physically, a near time span approach responds to the initial stage of stratified turbulence evolution when a gravity force only effects the largest eddies in a flow. According to obtained approximate solutions, the influence of stratification reveals itself in oscillations imposed on the smooth variance of the functions which are dependent only on the decreasing turbulence Reynolds number.

The usage of such an approach is justified by the fact that it enables one to find out satisfactory analytical solutions. On the other hand, it leads to less precise relations than the more common ones from [9] (see Figs. 1–5). As to the expression for turbulent mass flux, (14), the flux $\hat{q}_1$ was presented in a kind of a product of harmonic function $\hat{q}_1''(\tilde{\tau})$ to variable amplitude $\hat{q}_1'(t)$ without any additive components. It disagrees with the numerical run (see Fig. 6) and is the consequence of the fact that one of the equations of system (9) was dropped (namely, the fourth line) as it was inconsistent with the fifth line. Thus, one equation

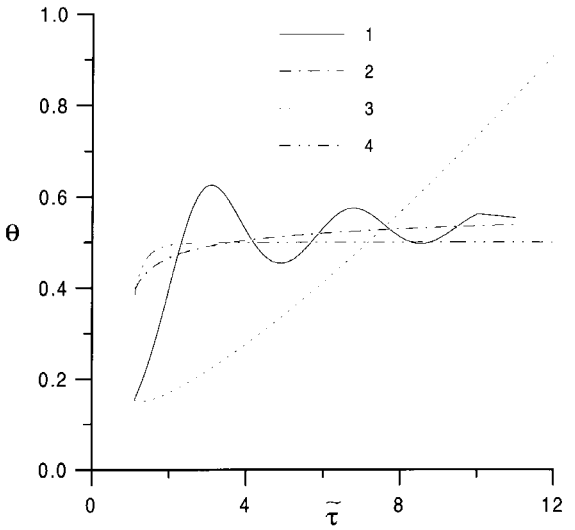

Fig. 5. Plot of various dependencies for the functions $\vartheta(\tilde{\tau})$ and $\hat{\vartheta}(\tilde{\tau})$: 1. ϑ in numerical computation by system (1); 2. $\hat{\vartheta}$ according to computation in [9]; 3. $\hat{\vartheta}$ according to formula (23); 4. $\hat{\vartheta}$ according to (24).

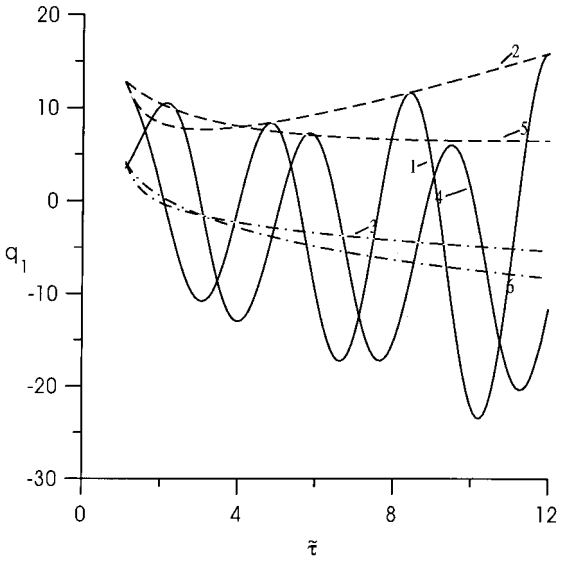

Fig. 6. Comparison of various dependencies for turbulent mass flux in near time span approach and in [9].

disappeared from the system together with an addition function—the additive component of turbulent mass flux.

To improve the drawback it may pass again to the variable $q = Fr\ q_1$ in the equation for turbulent mass flux after finding out approximation solutions for the other functions of the model and to split the equations on exponents of the small Fr number according to the same scheme, thus obtaining for the mass flux, a more precise presentation with a nonzero smooth component

$$q_1 = -\hat{c}_1/(Fr\,\hat{c}_2) + \hat{q}_1'\ \sin(\omega\tilde{\tau} + \phi_0). \tag{26}$$

In Fig. 6 the comparison is made between (26) and the numerical solution (curves 1 and 4, correspondingly). For both of them the wave-averaged dependencies calculated according to the algebraic formula

$$\hat{q}_1 = -\hat{c}_1/(Fr\,\hat{c}_2) \tag{27}$$

are also plotted (curves 3 and 6), where the coefficients $\hat{c}_1$ and $\hat{c}_2$ are taken from the approximate solutions (16), (17), (20) and (24) (curve 3) and from a more precise analysis [9] (curve 6). Rounded curves (2 and 5) for both variants are built with the formula: $q_1 = -\hat{c}_1/(Fr\,\hat{c}_2) + \hat{q}_1'$.

Summing up the results of the above comparisons note that the dependencies for the functions $\hat{R}$, $\hat{K}$, $\hat{E}$, $\hat{d}$ in near time span approach, fit the true evolution satisfactorily. The use of the high turbulence Reynolds number approach ($\hat{d} \ll 1$) leads to significant errors, caused mainly by the difference between the true dependence $\mathrm{d}(t)$ and the asymptotic law of 'one-fifth', (22). It is proved by the fact that the dependencies on $\hat{d}$ in common cases (16)–(18) and in the case of $d \ll 1$, (22), differ slightly (see Fig. 7).

For the functions ϑ and q_1 algebraic dependencies (24), and (27) agree very well with numerical solutions immediately from the initial conditions. For these functions an alternative specific approach taking initial conditions into consideration, such as formulae (19), and (23), is applicable only at a very short time interval.

4. Asymptotic expansion at an arbitrary Froude number

In this section we shall extend the previous analysis. First, the case of a Froude number, which is not small, will be considered. One more extension will deal with the treatment of another stratified turbulence model by the same asymptotic procedure.

To simplify the differential system (1) the following set of dimensionless variables is introduced

$$q = Fr^2\ T_\rho Q/E, \quad \vartheta = Fr^2\ \theta/E, \quad K = R_{22}/E$$

$$R = T_u/T_\rho, \quad t_1 = Fr\ T_\rho, \quad \tilde{\tau} = Fr \cdot \tau = N\tau^*. \tag{28}$$

In the case of an arbitrary Froude number this set of

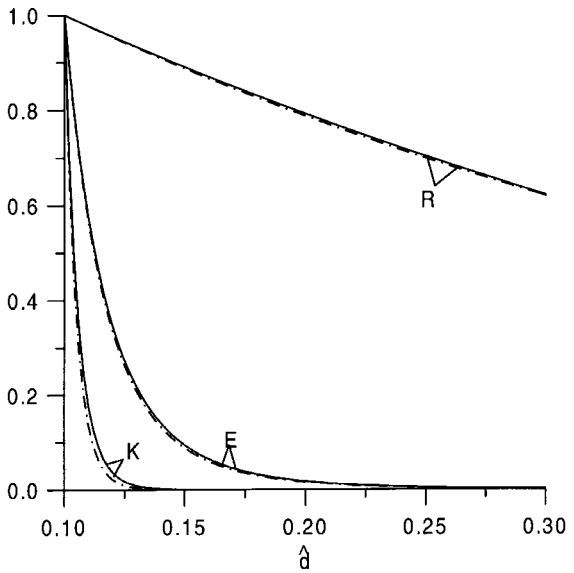

Fig. 7. Comparison of power dependencies (16)–(18) for the functions $(1/\hat{R}-1/R_\infty)(1/R_0-1/R_\infty) = f_R(\hat{d})$, $(\hat{K}-1/3)/(K_0-1/3) = f_K(\hat{d})$, $\hat{E}/E_0 = f_E(\hat{d})$, with asymptotic formulae in the case of $d \ll 1$, (22).

variables is more convenient since it enables one to exclude this number from the system. Varying a linear scale M and a velocity scale U in the definitions of non-dimensional variables we can set the Froude number to any value. For example, let us suppose new scales to be $U' = Uk$ and $M' = M/k$. It varies the Froude number $Fr' = Fr/k^2$ and the Reynolds numbers Re, Re_λ and the main variables R, q, K, ϑ, d, t_1, $\tilde{\tau}$ remain unchanged. Looking carefully at the analysis of [9], where the infinitesimal of the Fr was used, one can note that it was applicable when a small order of the Fr number in the equations did not interfere with the order of the variable $t = Fr^2\ T_\rho$. In other words, besides the condition $Fr \ll 1$ another condition $t \gg Fr$ (or $t_1 \gg 1$ in terms of this section variable) should also be satisfied. In this section we shall apply the asymptotic expansion procedure only for the condition $t_1 \gg 1$. In comparison with the parametric expansion on the small Fr number used in [9] this is a slightly more common case of coordinate expansion.

In view of designations (28) system (1) can be rewritten as

$$
\begin{aligned}
t_1 \frac{\mathrm{d}K}{\mathrm{d}\tilde{\tau}} &= \frac{-7d'(K-1/3)}{R} + 2q(K-4/5),\\
t_1 \frac{\mathrm{d}R}{\mathrm{d}\tilde{\tau}} &= \frac{4}{5} d(1 - R/R_\infty) - 2q(1-\alpha_2 R)R,\\
t_1 \frac{\mathrm{d}\vartheta}{\mathrm{d}\tilde{\tau}} &= 2\left(\frac{1}{R} - 1\right)\vartheta + 2q(1+\vartheta),\\
t_1 \frac{\mathrm{d}q}{\mathrm{d}\tilde{\tau}} &= t_1^2 A_1 + q\left[\frac{1}{R}\left(2 - \frac{d'}{3}\right) - 10d'K - \alpha_1 + p\right] + 2q^2,\\
\frac{\mathrm{d}t}{\mathrm{d}\tilde{\tau}} &= \frac{4d}{5R_\infty} + \frac{5d'}{3R} \equiv p,\\
t_1 \frac{\mathrm{d}E}{\mathrm{d}\tilde{\tau}} &= -\frac{2E}{R} - 2qE,
\end{aligned}
\tag{29}
$$

where designations for α_1, α_2, R_λ, σ, A_1 coincide with those in the previous section.

The additional equation for the function d is as follows:

$$
t_1 \frac{\mathrm{d}(d)}{\mathrm{d}\tilde{\tau}} = p_1\left(\frac{F_u^{**} - 4}{R} - 2(2 - \alpha_2 R)q\right). \tag{30}
$$

Introducing the new independent variable ξ from the relation

$$
\frac{\mathrm{d}\xi}{\mathrm{d}\tilde{\tau}} = \frac{1}{t_1} \tag{31}
$$

we shall seek an approximate solution of system (29)–(30) as a function of two 'independent' variables, 'slow' variable ξ and 'fast' variable $\tilde{\tau}$. Assuming the value of t_1 to be large, we shall construct the expansion of system (29) and (30) on exponents of $1/t_1$ in the following form

$$
\begin{aligned}
f &= \hat{f}(\xi, \tilde{\tau}) + \frac{\tilde{f}(\xi, \tilde{\tau})}{t_1^2} + \cdots,\\
q &= \hat{q}(\xi, \tilde{\tau}) + \frac{\tilde{q}(\xi, \tilde{\tau})}{t_1} + \cdots,
\end{aligned}
\tag{32}
$$

where f is one of the functions K, R, ϑ, d, E. We consider that the initial conditions are those, that $t_{10} \gg 1$. Since $p > 0$, the function t_1 grows monotonously, so the condition $t_1 \gg 1$ may be wrong only with some initial time span.

Considering that the functions in (29) depend on two variables $\tilde{\tau}$ and ξ, we shall substitute their decomposition (32) into (29). As a result the first equation of (29) can be written as

$$
\begin{aligned}
t_1 \frac{\partial \hat{K}}{\partial \tilde{\tau}} + \frac{\partial \hat{K}}{\partial \xi} + \frac{1}{t_1}\frac{\partial \hat{K}}{\partial \tilde{\tau}} &= \frac{-7\hat{d}'(\hat{K} - 1/3)}{\hat{R}}\\
&\quad + 2\hat{q}\left(\hat{K} - \frac{4}{5}\right) + \frac{1}{t_1} 2\tilde{q}\left(\hat{K} - \frac{4}{5}\right).
\end{aligned}
\tag{33}
$$

Decomposition of all other equations in (29), except that for q, is similar. Expansion in the equation for q has the following form

$$
\begin{aligned}
t_1 \frac{\partial \hat{q}}{\partial \tilde{\tau}} + \frac{\partial \hat{q}}{\partial \xi} + \frac{\partial \tilde{q}}{\partial \tilde{\tau}} + \frac{1}{t_1}\left(\frac{\partial \tilde{q}}{\partial \xi} - \hat{p}\tilde{q}\right)\\
= t_1^2 \hat{A}_1 + \tilde{A}_1 + \hat{q}\hat{c}_3 + 2\hat{q}^2 + \frac{\tilde{q}}{t_1}(\hat{c}_3 + 4\hat{q}).
\end{aligned}
\tag{34}
$$

Equalling the terms with identical exponents of t_1 in (33) and (34), we get:

—at t_1^2

$$
\hat{A}_1 = \hat{K} + \hat{\vartheta}[\hat{d}(\hat{K} - 1/3) - 2/3] = 0; \tag{35}
$$

—at t_1

$$
\frac{\partial \hat{K}}{\partial \tilde{\tau}} = 0, \quad \frac{\partial \hat{R}}{\partial \tilde{\tau}} = 0, \quad \frac{\partial \hat{\vartheta}}{\partial \tilde{\tau}} = 0, \quad \frac{\partial \hat{d}}{\partial \tilde{\tau}} = 0, \quad \frac{\partial \hat{q}}{\partial \tilde{\tau}} = 0; \tag{36}
$$

—at t_1^0 taking (36) into account

$$
\frac{\mathrm{d}\hat{K}}{\mathrm{d}\xi} = -\frac{7(1-\hat{d})(\hat{K} - 1/3)}{\hat{R}} + 2\hat{q}(\hat{K} - 4/5), \tag{37}
$$

$$\frac{\mathrm{d}\hat{R}}{\mathrm{d}\xi} = \frac{4}{5}\hat{d}(1-\hat{R}/R_\infty) - 2\hat{q}\hat{R}(1-\alpha_2\hat{R}), \tag{38}$$

$$\frac{\mathrm{d}\hat{\vartheta}}{\mathrm{d}\xi} = 2(\hat{R}^{-1}-1)\hat{\vartheta} + 2\hat{q}(1+\hat{\vartheta}) \tag{39}$$

$$\frac{\mathrm{d}(\hat{d})}{\mathrm{d}\xi} = \frac{\hat{d}(1-\hat{d})}{1+\hat{d}}\left[\left(\frac{1}{3}+\frac{13}{15}\hat{d}\right)\hat{R}^{-1} + 2\hat{q}(2-\alpha_2\hat{R})\right], \tag{40}$$

$$\frac{\partial\tilde{q}}{\partial\tilde{\tau}} = \tilde{A}_1 + f(\xi), \tag{41}$$

where $f(\xi) = -(\mathrm{d}\hat{q}/\mathrm{d}\xi) + \hat{q}\hat{c}_3 + 2\hat{q}^2$;
—at t_1^{-1}

$$\frac{\partial\tilde{K}}{\partial\tilde{\tau}} = 2(\hat{K}-4/5)\tilde{q}, \tag{42}$$

$$\frac{\partial\tilde{R}}{\partial\tilde{\tau}} = -2\hat{R}(1-\hat{\alpha}_2\hat{R})\tilde{q}, \tag{43}$$

$$\frac{\partial\hat{\vartheta}}{\partial\tilde{\tau}} = 2(1+\hat{\vartheta})\tilde{q}, \tag{44}$$

$$\frac{\partial\tilde{d}}{\partial\tilde{\tau}} = -2\hat{p}_1(2-\hat{\alpha}_2\hat{R})\tilde{q}, \tag{45}$$

$$\frac{\partial\tilde{q}}{\partial\xi} = \tilde{q}(\hat{c}_3 + \hat{p} + 4\hat{q}). \tag{46}$$

Differentiating relation (35) we get

$$\frac{\mathrm{d}\hat{A}_1}{\mathrm{d}\xi} = (\hat{c}_1 + \hat{c}_2\hat{q}) = 0,$$

whence it follows the algebraic equation for the wave-averaged vertical mass flux

$$\hat{q} = -\frac{\hat{c}_1}{\hat{c}_2}. \tag{47}$$

This wave-averaged mass flux is caused by internal wave motion. In order to satisfy the continuity condition another mass flux should exist not described by the homogeneous turbulence equations. It is equal to that given in (47) by absolute value and opposite in direction. Relation (47) gives the ground to calculate that known from the experimental works counter-flux which occurs at small scales.

Relation (47) is a consequence of Eqs. (35)–(40). If we intend to take the usage of (47) one of the differential equations in (35)–(40) should be omitted to avoid this system being overdetermined. As was done in the previous section we shall determine the variable $\hat{\vartheta}$ from the algebraic Eq. (35) and omit the differential equation for this variable, (39). The system of the two algebraic equations (35) and (47) and the three differential equations, (37), (38) and (40), describes wave-averaged behavior of the functions in system (29). Below we shall refer to this system, which serves to determine the functions with 'hats', as to system (A).

The following group consists of five equations (41)–(45) (system (B)). It describes the dependence of functions on $\tilde{\tau}$. The function $\hat{q}(\xi)$ in (41) should be considered as being known, since it has been determined by formula (47). Differentiating (41) partially over $\tilde{\tau}$ we obtain a wave equation for $\tilde{q}$

$$\frac{\partial^2\tilde{q}}{\partial\tilde{\tau}^2} = \frac{\partial}{\partial\tilde{\tau}}\tilde{A}_1 = 2\hat{c}_2\tilde{q}.$$

The general solution of this equation can be written as

$$\tilde{q} = \tilde{q}'(\xi)\sin\ \phi \tag{48}$$

where $\phi = \omega(\xi)\tilde{\tau} + \phi_0(\xi)$, $\omega = \sqrt{-2\hat{c}_2}$.

Presenting other functions with tildes in Eqs. (42)–(45) as the products

$$\tilde{K} = \tilde{K}'(\xi)\cos\ \phi, \quad \tilde{R} = \tilde{R}'(\xi)\cos\ \phi,$$

$$\tilde{\vartheta} = \tilde{\vartheta}'(\xi)\cos\ \phi, \quad \tilde{d} = \tilde{d}'(\xi)\cos\ \phi \tag{49}$$

and substituting (48), we get the relations between amplitudes

$$\tilde{K}' = -2\left(\hat{K}-\frac{4}{5}\right)\frac{\tilde{q}'}{\omega}, \quad \tilde{R}' = 2\hat{R}(1-\hat{\alpha}_2\hat{R})\frac{\tilde{q}'}{\omega},$$

$$\tilde{\vartheta}' = -2(1+\hat{\vartheta})\frac{\tilde{q}'}{\omega}, \quad \tilde{d}' = 2\hat{p}_1(2-\hat{\alpha}_2\hat{R})\frac{\tilde{q}'}{\omega}. \tag{50}$$

According to relations (49) the functions $\tilde{K}$, $\tilde{R}$, $\tilde{\vartheta}$, $\tilde{d}$ oscillate under the cosine law and the function $\tilde{q}$ under the sine law. The amplitudes of oscillations (50) are proportional to the amplitude of vertical mass flow oscillation $\tilde{q}'$. The similar relations can be obtained for turbulence kinetic energy E. Applying a small parameter decomposition procedure in a form of (32) to the equation for E in (29) results in the following equations for zero and first-order approaches accordingly

$$\frac{\mathrm{d}\hat{E}}{\mathrm{d}\xi} = \frac{-2\hat{E}}{\hat{R}}, \quad \frac{\partial\tilde{E}}{\partial\tilde{\tau}} = -2\hat{E}\tilde{q}. \tag{51}$$

In (51), presenting the function in a form of a product $\tilde{E}(\xi,\tilde{\tau}) = \tilde{E}'(\xi)\cos\ \phi$, for the amplitude of turbulence kinetic energy oscillation we obtain $\tilde{E}'(\xi) = 2\hat{E}\tilde{q}'/\omega$.

To find out the amplitude of vertical mass flow oscillation, let us refer to Eq. (46). Substituting the relation (48) here gives

$$\frac{d\tilde{q}'}{d\xi} = \tilde{q}'(\hat{c}_3 + \hat{p} + 4\hat{q}). \tag{52}$$

It follows from system (B) that, as in the previously considered case of a small Froude number, [9], the oscillations in the far region are nearly harmonic: these are the sine waves with the frequency and amplitudes dependent on ξ. The amplitude of $\tilde{q}$-oscillations, $\tilde{q}'(\xi)$, can be calculated from the ordinary differential equation (52), all the other amplitudes are related to $\tilde{q}'$ with algebraic ties (50). The phase of $\tilde{q}$-oscillations is shifted to a quarter of the period to that of the other functions.

Considering subsystem (A) one can note that the functions with 'hats' depend only on 'slow' variable ξ. Two equations of this subsystem are algebraic. It means that at some initial point only three initial conditions from five, say $\hat{K}_0$, $\hat{R}_0$, $\hat{d}_0$, determine the subsequent evolution of mean values. Depending on the chosen initial set of parameters $\hat{K}_0$, $\hat{R}_0$, $\hat{d}_0$, we obtain the different laws of evolution and the different final states of turbulence at $\tilde{\tau}\to\infty$.

System (A) was investigated for infinity time. First, stationary solutions of (A) were found. Doing so, an algebraic system resulting from the derivatives on the left-hand-side of (A) equalling zero was reduced to a single transcendental equation which was then solved numerically. All the solutions having a physical sense ($\hat{K}$, $\hat{d}\in(0, 1)$, $\hat{R}$, $\hat{\vartheta}\geq 0$) were considered. It was found that together with that obtained earlier in [10] an

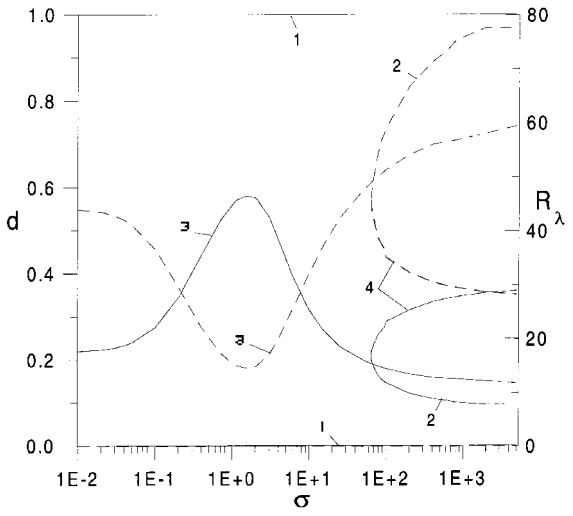

Fig. 8. Parameter $d(R_\lambda^2)$ (left axis, solid curves) and turbulence Reynolds number R_λ (right axis, dashed curves) versus Prandtl number σ for the various asymptotic branches.

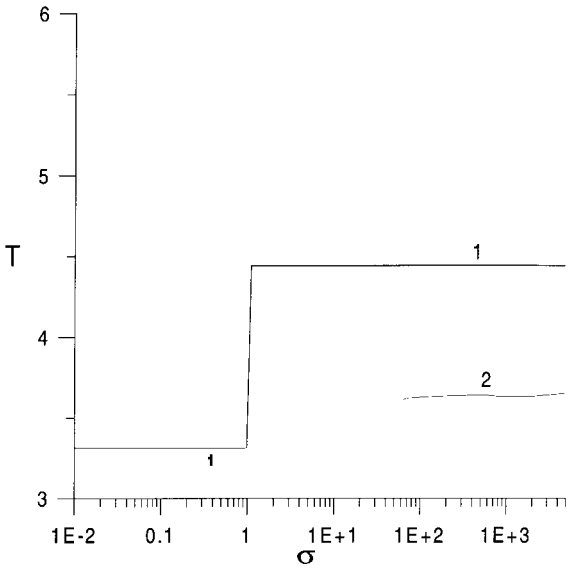

Fig. 9. Period of internal gravity waves T versus Prandtl number σ for asymptotic branches 1 and 2.

asymptotic mode in which the turbulent Reynolds number $R_\lambda \to 0$ at $\tilde{\tau} = \infty$, there is another asymptotic mode for which R_λ const at infinity time (see Fig. 8, branches 2–4). The numerical solution of subsystem (A) for different sets of initial conditions supported the prediction from the stationary analysis existence of an asymptotic mode with $R_\lambda \to$ const and let us determine that these are branches 1 and 2 which are realised at infinity time. Since the asymptotic branches 3 and 4 in Fig. 8 were not detected in the numerical solution of the non-stationary problem, they are omitted in the subsequent figures. Mode 1 at $\sigma > 1$ represents the fossilisation regime ($K = 0.8$), while Mode 2 responds to the asymptotic state with a large turbulent Reynolds number and very close to isotropy ($K = 0.35$).

The second mode only appears at large Prandtl numbers ($\sigma > 64$). For this one the period of internal gravity waves (Fig. 9) is close to that of 3.6 and nearly constant. The value of T which corresponds to the first (fossilisation) mode at $\sigma > 1$ proved to be noticeably higher, $T \approx 4.3$. Other characteristics of the second mode take an intermediate position between analogous functions for Mode 1 at $\sigma < 1$ and $\sigma > 1$ as well. The behavior of the time scale ratio (Fig. 10) is an exception. With an increasing Prandtl number the ratio R/R_∞ increases to three. It is much more than that for Mode 1 for all ranges of σ. The scale ratio R reaches the value 0.62 at $\sigma \gg 1$. The rate of TKE decay for Mode 2 (Fig. 10) exceeds that for Mode 1, but, at the same time it is noticeably less than the characteristic exponent of 2.5 peculiar for Mode 1 at $\sigma < 1$. For both modes at $\sigma > 1$ the ratio of the kinetic energy of

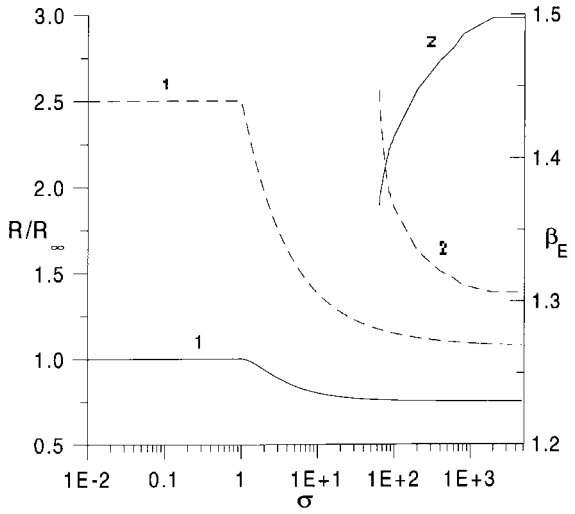

Fig. 10. Asymptotic ratio R/R_∞ (left axis, solid curves) and the exponent in power law of TKE decay β_E (right axis, dashed curves) for asymptotic branches 1 and 2 versus Prandtl number σ.

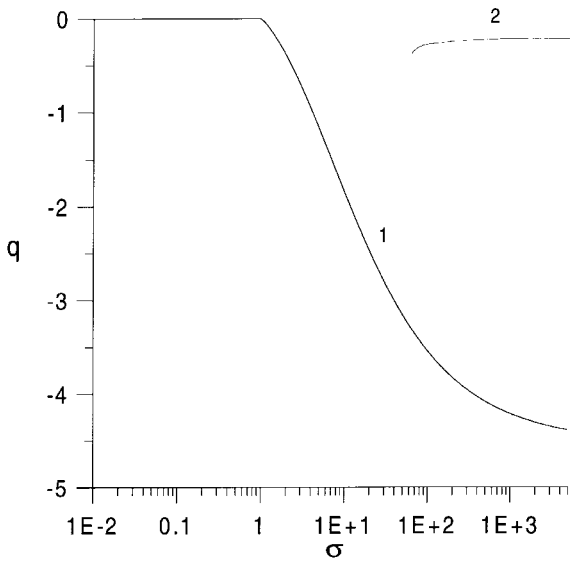

Fig. 12. The dependence of dimensionless vertical mass flux q on Prandtl number σ for branches 1 and 2 of asymptotic solution.

the vertical velocity fluctuation to the potential energy of density fluctuation K/ϑ differs from unity, the value usual for pure linear oscillations (see branch 1 at $\sigma < 1$, Fig. 11).

Mode 1 at $\sigma < 1$ thus, represents the special linear case of oscillations. It is the only branch, where the wave-averaged vertical flux $\hat{q}$ is zero in the final stage (Fig. 12). It can also be demonstrated by comparing the amplitudes of waves $\tilde{f}'$ with the corresponding mean values, $\hat{f}$. In contrast to the other branches, for this mode (Mode 1 at $\sigma < 1$) the amplitudes decrease more slowly than mean values. Branches 1 and 2 at $\sigma < 1$ are similar to some extent. They both correspond to the absence of significant influences of stratification in the final stage of turbulence decay (see Fig. 12). In some other aspects they are also alike (Figs. 9 and 13). Nevertheless, an essential difference between

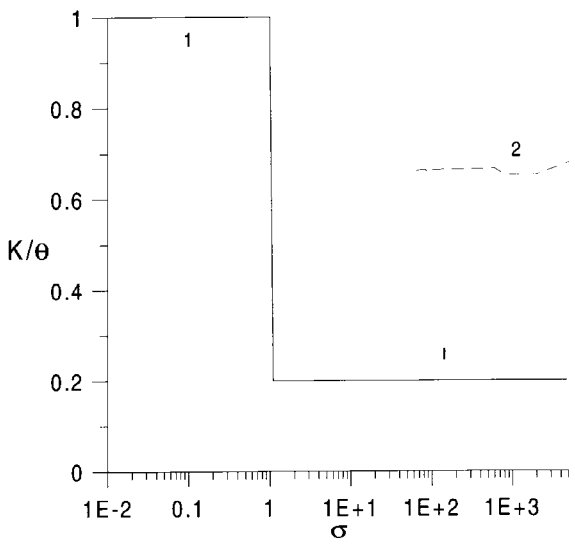

Fig. 11. The ratio of kinetic energy of vertical velocity fluctuations to potential energy of density fluctuation for two asymptotic modes at various Prandtl numbers.

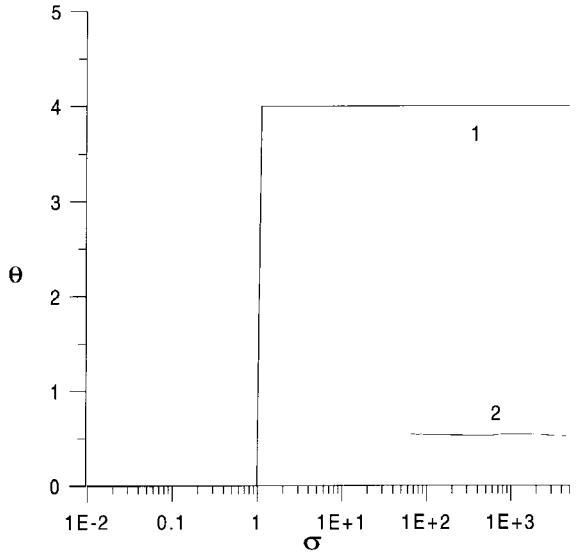

Fig. 13. The ratio of potential energy of density fluctuations to TKE, θ, for branches 1 and 2 of asymptotic solution versus molecular Prandtl number σ.

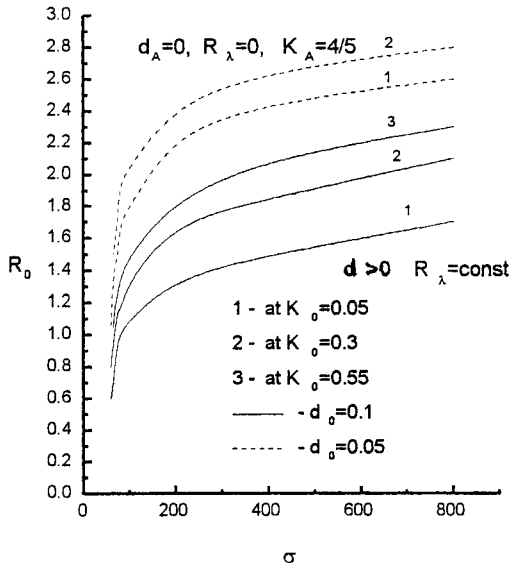

Fig. 14. Map of the area of initial conditions R_0, K_0 leading to asymptotic branches with $R_\lambda \to 0$ (space above the curves) and $R_\lambda \to \text{const}$ (space below the curves) for $d_0 = 0.1$ and $d_0 = 0.05$.

the two modes is formed by the fact that the turbulence Reynolds number tends to zero for the former and remains high for the latter.

At any molecular Prandtl/Schmidt number σ the initial area of state for wave-averaged functions $\hat{f}$ is defined only by the three initial conditions $\hat{K}_0$, $\hat{R}_0$, $\hat{d}_0$. Depending on these three parameters the solution of (A) tends to different asymptotic limits, described in Figs. 8–13. The differential system (A) was solved with Gear's method for various initial data sets. For initially strong turbulence ($\hat{d}_0 = 0.1$) Fig. 14 shows the obtained map of initial states leading to one ($R_\lambda \to 0$, the area above the lines) or another ($R_\lambda \to \text{const}$, the area below the lines) final mode. As one can see, the asymptotic mode with $R_\lambda \to \text{const}$ can only be realized at high values of the molecular Prandtl number ($\sigma > 10.5$). At low values of $\hat{d}_0$ (at $\hat{d}_0 = 0.05$ and especially at $\hat{d}_0 = 0.03$) the curves separating these two areas are almost vertical with the small dependence on $\hat{K}_0$.

The first mode ($R_\lambda \to 0$) corresponds to fossil turbulence in a final stage when more energy is in a potential form and a gravity wave dissipates slowly. The essence of this regime was described in detail in [10], where the asymptotic laws of evolution were deduced. The area of initial states tending to this mode is shrunk with the growth of σ and K_0 as well as with the lowering of d_0. In a fossil mode dissipation is lower than for branch 2, which is similar to a passive scalar case. Various scenarios of turbulence decay in stratified media depending on a set of initial parameters have also been pointed out in published experimental works.

To complete the description of two-scale decomposition it is necessary to determine the coordinate ξ and the function $t(\xi, \tilde{\tau})$. These values can be calculated from differential equations

$$\frac{\mathrm{d}t}{\mathrm{d}\tilde{\tau}} = p = \frac{4d}{5R_\infty} + \frac{5(1-d)}{3R}, \quad \frac{\mathrm{d}\xi}{\mathrm{d}\tilde{\tau}} = \frac{1}{t_1} \tag{53}$$

where the functions $d(\xi(\tilde{\tau}), \tilde{\tau})$ and $R(\xi)\tilde{\tau}), \tilde{\tau})$ are given by two terms of decompositions (32)

$$d(\tilde{\tau}) = \hat{d}(\xi) + \frac{\tilde{d}'(\xi)\cos(\omega(\xi)\tilde{\tau})}{t_1^2},$$

$$R(\tilde{\tau}) = \hat{R}(\xi) + \frac{\tilde{R}'(\xi)\cos(\omega(\xi)\tilde{\tau})}{t_1^2}.$$

At a large t_1 system (53) can be solved approximately. Expanding the functions p and t_1 into the series up to terms of the order $1/\hat{t}_1^2$

$$p = \hat{p} + \frac{\tilde{p}}{\hat{t}_1^2} + \cdots, \quad t_1 = \hat{t}_1 + \frac{\bar{t}}{\hat{t}_1} + \frac{\tilde{t}}{\hat{t}_1^2} \ldots,$$

and combining the terms with identical exponents of $\hat{t}_1$ we have the following set of equations

$$\frac{\mathrm{d}\hat{t}_1}{\mathrm{d}\tilde{\tau}} = \hat{p}(\xi), \quad \frac{\mathrm{d}\bar{t}}{\mathrm{d}\tilde{\tau}} = 0,$$

$$-\bar{t}\hat{p}(\xi) + \frac{\mathrm{d}\tilde{t}}{\mathrm{d}\tilde{\tau}} = F(\xi)\cos(\omega(\xi)\tilde{\tau}),$$

where

$$F(\xi) = \frac{\mathrm{d}\hat{p}}{\mathrm{d}\hat{R}}\tilde{R}'(\xi) + \frac{\mathrm{d}\hat{p}}{\mathrm{d}(\hat{d})}\tilde{d}'(\xi)$$

$$= \left(-\frac{5(1-\hat{d})}{3\hat{R}^2}\right)\tilde{R}'(\xi) + \left(\frac{4}{5R_\infty} - \frac{5}{3\hat{R}}\right)\tilde{d}'(\xi).$$

Since the derivative $\mathrm{d}\xi/\mathrm{d}\tilde{\tau} = 1/t_1$ is small the function $\hat{p}(\xi)$ and $F(\xi)$ in (54) can be thought of as being constant. So the approximation solution of (54) is

$$\hat{t}_1 = \hat{t}_{10} + \hat{p}(\tilde{\tau} - \tilde{\tau}_0), \quad \bar{t} = \bar{t}_0,$$

$$\tilde{t} = \tilde{t}_0 + \bar{t}_0\hat{p}\tilde{\tau} + (F/\omega)\sin(\omega\tilde{\tau}).$$

As a result, the expression for $t_1(\tilde{\tau})$ takes the following form

$$t_1 = \hat{t}_1 + \frac{\bar{t}_0}{\hat{t}_1} + \frac{\tilde{t}_0 + \bar{t}_0\hat{p}\tilde{\tau}}{\hat{t}_1^2} + \frac{(F/\omega)}{\hat{t}_1^2}\sin(\omega\tilde{\tau}). \tag{55}$$

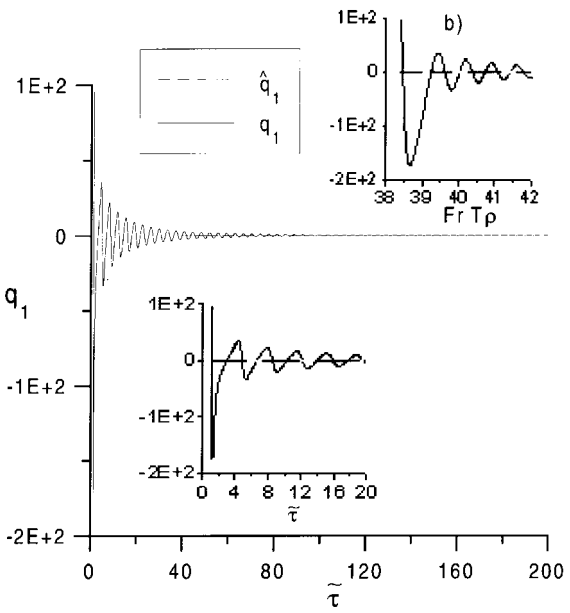

Fig. 15. Time evolution of vertical mass flux $q_1 = q/Fr^2$ in comparison with the evolution of averaged flux $\hat{q}_1$ in initial part of trajectory; (a) $q_1 = q_1(\tilde{\tau})$, (b) $q_1 = q_1(Fr\ T_\rho)$.

The first term in (55) describes a linear growth of t_1 with $\tilde{\tau}$, the second and third ones describe deflection from the linear behavior of $t_1(\tilde{\tau})$, and the fourth—the oscillations imposed on the smooth variance of the function. The numerical solution of the differential system (1) fully supports the obtained law (55). Comparing (55) with this numerical solution we were able to determine the values of constants $\hat{t}_0$, $\bar{t}_0$ and $\tilde{t}_0$.

Expression (55) together with the previously obtained approximate solutions in the form (32) shows that at large t_1 oscillations in a stratified flow have a pure sine form, as it has been pointed out in [9], but at a moderate t_1 the form of oscillation is more complex and depends on the relative values of amplitudes of oscillations in the numerator and the denominator of the second term in (32). Figs. 15 and 16, where the results of numerical solution of (1) are plotted, illustrate the issue.

In these figures all the initial conditions and parameters were the same as in the previous section except that of the Froude number being replaced with a rather large value of $Fr = 1$. In terms of our main variables (28) it changes the initial conditions for the two functions, q_0 and ϑ_0. The effect of such a replacement is the same as decreasing the variable E, because it enters into the definitions of both. Thus, this extreme case corresponds to the situation when total energy is mostly contained in the potential energy of density fluctuations.

As the interaction of internal gravity waves and irregular turbulent fluctuations is critically important for prescribing stratified flows, the information on what terms and to what extent these are responsible for the wave amplitude, frequency and decay laws can be useful in modeling and comparison of specific features of different turbulent models. A review of the modern second-order turbulence models capable of adequately describing a stratified turbulence [8] shows that the structure of them is definitely close to the structure of system (1). In particular, a number of algebraic relations is proposed for the transverse turbulent mass flux. It has been noted, [8], that such algebraic relations in models lead to excluding internal gravity waves from consideration. Naturally, present analysis supports this point of view to mass flux oscillations as a generator of oscillations in all other functions of the model. Investigation by small parameter methods clearly shows the role of algebraic relations (for the variables q and ϑ) as averaging over the internal wave oscillation.

The method developed in this study can be almost repeated for other models of stratified homogeneous turbulence. For example, let us consider the model in [15] which is the baseline one in the compatible analysis of stratified turbulence models in [8]. As the numerical experiments by DNS [16] has shown, this model is able to predict the amplitude and period of internal gravity waves. The structure of this model, [15], is very similar to that of system (1) with the exception that some constants of the model in [15] are

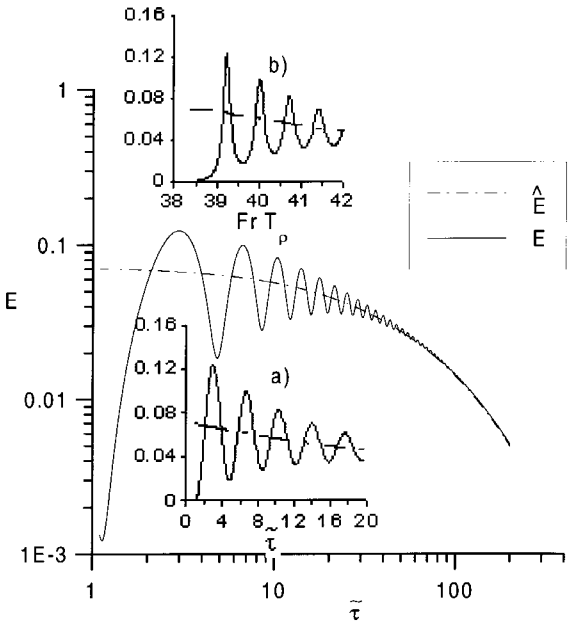

Fig. 16. Time evolution of TKE in comparison with the evolution of averaged energy $\hat{E}$. (a), (b) Initial part of trajectory; (a) $E = E(\tilde{\tau})$, (b) $E = E(Fr\ T_\rho)$.

Table 1
Differences between systems (1) and (1)–(8) from [15]

Model [6]	Model [15]
$F_u^{**}/2 = \frac{11}{6} - \frac{13}{30}d$	$C_{\epsilon 2} = 1.83$
$d[2\sigma/(1+\sigma)](\sigma_\infty + 3/5)(R/R_\infty)$	$C_{\epsilon 3} = \frac{3}{2}$
$\frac{9}{2}(1-d)+d$	$C_1 = \frac{3}{2}$
$\frac{1}{3} + d(K - \frac{1}{3})$	$C_{2\theta} = 0.4$
$(1-d)(\frac{1}{6} + 5KR) + d(\sigma_\infty + \frac{3}{5})(R/R_\infty)$	$C_{1\theta} = 3$
$2 + \frac{4}{5}(d/R_\infty)$	$C_{d4} = 2.2$
$\frac{5}{6}(1-d)$	$C_{d5} = 0.8$
2	$C_{d1} = 1.8$

replaced with the functions from the turbulent Reynolds number and the Prandtl number in (1). After the term-by-term comparison of Eqs. (1)–(8) from [8] (model LS/MTS, [15]) and Eqs. (1) of this paper (model Ref. [6]) the differences between them can be summarized in the following Table.

Looking at Table 1, one can see that many of the terms from both the columns at $d = 0$ are very close to each other. If it were so in every equation, the terms in the left column may be reasonably considered as a universal extension of the right column terms to the variance of *Re* and *Pr* numbers (remember that the equations of the model in [6,12] were deduced demanding such a universality). Unfortunately, there are also significant disturbing differences to make such a conclusion, namely in the second, third and fifth lines of the table. Probably, the most obvious difference is in the third line, with the value of constant $C_1 = 1.5$ being three times lower than the value of the corresponding terms in the left column at $d = 0$. The matter needs to be studied further taking into account that the value of constant $C_1 \simeq 1.5$ is rather common.

Being expressed through the variables (28), the equations in [15] look very similar to system (29)

$$t_1\,\mathrm{d}K/\mathrm{d}\tilde{\tau} = 2(1-C_1)(K-1/3)R^{-1} + 2q(K-4/5),$$

$$t_1\,\mathrm{d}R/\mathrm{d}\tilde{\tau} = 2(C_{\epsilon 2}-1) - 2C_{d5} - R(C_{d4}-2) - 2qR(1 - C_{\epsilon 3} - (C_{d1}-2)/(2\vartheta)),$$

$$t_1\,\mathrm{d}\vartheta/\mathrm{d}\tilde{\tau} = 2(R^{-1}-1)\vartheta - 2q(1+\vartheta),$$

$$t_1\,\mathrm{d}q/\mathrm{d}\tilde{\tau} = t_1^2[K - \vartheta(1-C_{2\theta})] + [C_{d4} - 2 + 2R^{-1} \times (1 + C_{d5} - C_{1\theta})]q + (2 - (C_{d1}-2)\vartheta^{-1})q^2,$$

$$\mathrm{d}t_1/\mathrm{d}\tilde{\tau} = (C_{d4}-2) + 2C_{d5}R^{-1} - (C_{d1}-2)q\vartheta^{-1},$$

$$t_1\,\mathrm{d}E/\mathrm{d}\tilde{\tau} = -2ER^{-1} - 2qE, \qquad (56)$$

and can be analyzed at large t_1 by the same procedure of asymptotic expansion (32)–(34). Doing so, the equations of (56) are split into systems describing the wave-averaged behavior of functions [similar to (35), (37)–(40), and (47)], the internal waves [similar to (48)–(51)], and the variance of amplitude [analogous to (52)]. The system for wave-averaged functions after substituting the numerical values of the constants takes the following form:

$$t_1\,\mathrm{d}\hat{K}/\mathrm{d}\tilde{\tau} = -(\hat{K} - 1/3)\hat{R}^{-1} + 2\hat{q}(\hat{K} - 4/5),$$

$$t_1\,\mathrm{d}\hat{R}/\mathrm{d}\tilde{\tau} = 0.06 - 0.2\hat{R}(1 + \hat{q}/\hat{\vartheta}) + \hat{R}\hat{q},$$

$$\hat{q} = -\frac{5}{14\hat{R}}\left[\hat{K} - \frac{1}{3} + 2\hat{K}(1-\hat{R})\right],$$

$$t_1\,\mathrm{d}\hat{E}/\mathrm{d}\tilde{\tau} = -2\hat{E}(\hat{R}^{-1} + \hat{q}),$$

$$t_1\,\mathrm{d}(\hat{d})/\mathrm{d}\tilde{\tau} = \hat{p}_1[-0.34\hat{R}^{-1} - \hat{q}],$$

$$\hat{A} \equiv \hat{K} - 0.6\hat{\vartheta} = 0,$$

$$\mathrm{d}t_1/\mathrm{d}\tilde{\tau} = 0.2(1 + \hat{q}/\hat{\vartheta}) + 1.6\hat{R}^{-1}. \qquad (57)$$

Initial conditions for system (56) were based on those given in [8]: $K_0 = 1/3$, $R_0 = 1$, $q_0 = 0$, $\vartheta_0 = 2.415 \times 10^{-2}$, $E_0 = 1$, $d_0 = 5 \times 10^{-3}$, $t_{10} = 5.255$ with the exception that the condition for ϑ was slightly enlarged compared with [8], $\vartheta_0 = E_{\mathrm{pot}}/k = 10^{-2}/0.414 = 2.415 \times 10^{-2}$ for the reason that at lower values of E_{pot} the solution of the problem turned out to be sensitive to the variance of ϑ_0. Remember, that in contrast to [8] where the Runge–Kutta method was used, we used Gear's method for the integration of system (56). The initial condition for E could be chosen arbitrarily, so the value $E_0 = 1$ was taken. The value of parameter $d_0(R_{\lambda 0}^2) = 1 - 2/(1 + \sqrt{1 + 2800/R_{\lambda 0}^2})$ was calculated using the initial condition for the turbulent Reynolds number from [8], $R_{\lambda 0}^2 = 20 \times 6925 = 1.385 \times 10^5$. The initial conditions for the 'smoothed' system were adjusted to better represent the wave-averaged behavior of the functions: $\hat{K}_0 = 0.185$, $\hat{R}_0 = 0.9$, $\hat{\vartheta} = 0.43$, $\hat{E}_0 = 0.81$, $\hat{d}_0 = 7.4 \times 10^{-3}$.

The numerical solutions of systems (56) and (57) are compared in Figs. 17–19. As one can see, the solution of the 'smoothed' system (57) really describes the wave-averaged functions from (56). An agreement between them could be better if larger initial values of variable t_1 were taken. Nevertheless, even at a relatively low value of t_{10} the results of the comparison

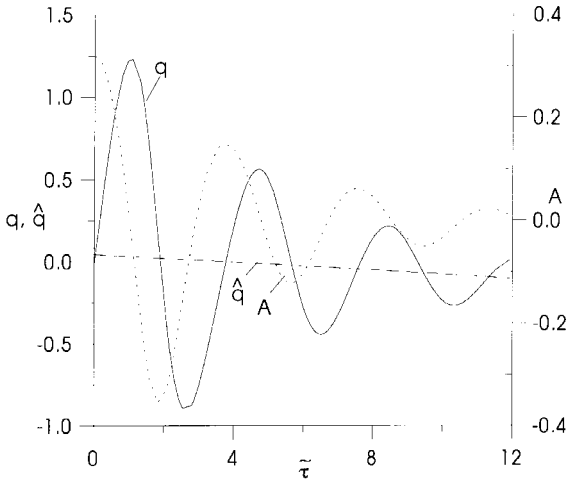

Fig. 17. Wave and wave-averaged turbulent mass flux q and function A, representing dynamic equilibrium between kinetic and potential energy in the model in [15].

support clearly the asymptotic analysis of this section. It is seen from Fig. 17, in particular, that the average value of a complex $\hat{A} = \hat{K} - 0.6\hat{\vartheta}$ is close to zero. It means that the relation $\hat{A} = 0$ really represents the dynamic equilibrium condition between the potential and kinetic energy of stratified turbulence during oscillations caused by gravity force. This relation is similar to that of $\hat{A}_1 = 0$ for the model in [6]. In the case of very strong turbulence ($d \ll 1$) the condition $\hat{A}_1 = 0$ looks like:

$$\hat{K} - \frac{2}{3}\hat{\vartheta} = 0.$$

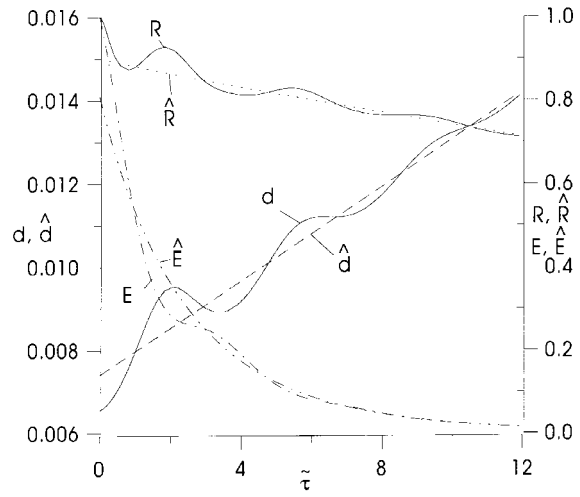

Fig. 18. Wave and wave-averaged behavior of TKE E, time scale ratio R, and turbulence Reynolds number parameter d in the model in [15].

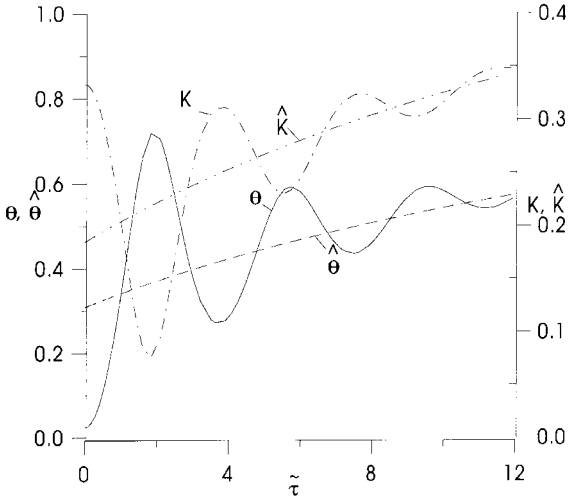

Fig. 19. Comparison of full and wave-averaged dependencies of ratios $\vartheta(\tilde{\tau})$ and $K(\tilde{\tau})$ calculated according to the model in [15].

The equation for the average value of vertical mass flux $\hat{q}$ in (57) is obtained by differentiating the condition $\hat{A} = 0$. It is also in good agreement with the calculated dependence $q(\tilde{\tau})$ (Fig. 17). Plots of $q(\tilde{\tau})$ and $A(\tilde{\tau})$ are shifted to a quarter of the period, the value of the period being prescribed in the analysis of (56) and (57) as a constant $N\tau = 2\pi/\omega = 2\pi/\sqrt{2(7/5)} = 3.75$. This numerical value coincides with that obtained by solving system (56) numerically and is close to that calculated by formulae (48) in an isotropic state at a strong turbulence ($d \ll 1$): $N\tau = 2\pi/\omega = 2\pi/\sqrt{-2(-4/5 - 2/3)} = 3.67$.

Since the considered initial conditions for the model in [15] are those that $d_0 \ll 1$ and $\hat{q}_0 = 0$, the wave-averaged values $\hat{d}$, $\hat{E}$ and $\hat{R}$ evolve in the initial stage of evolution (Fig. 18) in agreement with those prescribed in the previous laws section [see (22) and Figs. 1–3]. In particular, let us calculate the exponent in the evolution law of $\hat{d}(t_1)$, $\beta_{\hat{d}} = (t_1/\hat{d})[\mathrm{d}(\hat{d})/\mathrm{d}t_1]$. In the equations of the 'smoothed' model (57) at $\hat{q} = 0$ and $\hat{d} \ll 1$ this exponent is equal to: $\beta_{\hat{d}} = -[-0.34\hat{R}^{-1}]/(0.2 + 1.6\hat{R}^{-1})$. At $\hat{R} = 1$ it is very close ($\beta_{\hat{d}} = 0.189$) to the above prescribed 'one-fifth' law for $\hat{d}$, see (22). At these conditions the TKE decays with the rate $\beta_{\hat{E}} = (-2\hat{R}^{-1})/(0.2 + 1.6\hat{R}^{-1}) = -2/(0.2 + 1.6) = -1.11$ [see, for comparison, $\beta_{\hat{d}} = 1/5$, $\beta_{\hat{E}} = -6/5$ in (21)]. The evolution of $\hat{K}$ (Fig. 19) reveals much slower relaxation than in theory [6] due to a much lower coefficient at deviator $\hat{K} - 1/3$ on the right-hand-side of the equation for $\hat{K}$ from [5] than in (37).

In conclusion, it is interesting to investigate whether theory [15] lets the turbulent Reynolds number R_λ tend to a non-zero asymptotic value, as in theory [6].

To investigate this problem, the derivatives on the left-hand-side of (57) were equalled to zero, and the resulting algebraic stationary system was solved. Unfortunately, no stationary asymptotic solutions having physical sense were found this way, since model [15] did not pretend to describe the final stage of turbulence decay. So the existence of various asymptotic modes detected in this paper remains unsupported by the analysis of other models.

5. Conclusions

1. Using the model [6,12] of stratified homogeneous turbulence the initial stage of evolution has been considered analytically at a small inverse Froude number Fr and an initially strong turbulence $R_\lambda \gg 1$. This stage corresponds to a small wave-averaged turbulent mass flux $\hat{q}$ as compared with the oscillations of $q(\tau)$. Under these conditions the flux $\hat{q}$ behaves as a passive impurity and can be found after taking into account all the other functions in (9). The approximate analytical solutions (22) in the case of $d \ll 1$ and in a more common case (16)–(20), and (27) are in agreement with the numerically obtained results (Figs. 1–7). The initial stage of evolution is determined mainly by the variance of the turbulent Reynolds number.
2. The case of the arbitrary Froude number was studied at a large time scale of density field, T_ρ. The application of a small parameter method in combination with a multiple scales method let us formulate the mathematical systems, describing as regular oscillation, an averaged values variance. This analysis enables one to calculate the parameters of an internal gravity wave, namely the amplitude, frequency and wave-averaged behavior. According to this analysis the evolution of stratified turbulence can be treated as a non-linear (in common cases) internal gravity wave imposed on irregular turbulence fluctuations. The energy of this wave is borrowed from a density fluctuation field and a velocity fluctuation field, showing that the interaction of regular oscillations (gravity waves) and turbulent fluctuations can lead to different final states dependent on initial sets of variables (Fig. 13).
3. Analysis of the turbulence model [6] was supported by the analysis of the model in [15] from [8] with the same method. The parameters of both the models were compared. Some of them turned out to be very close to each other. Despite the relatively low initial value $T_{\rho 0}$, the numerical data of [8] agrees well with the asymptotic analysis of this paper. In particular, the frequency of internal gravity wave and wave-averaged behavior (Figs. 17–19) coincided with those in the numerical data of [8].

The analytical expressions of the developed analysis clearly shows the influence of various constants of the models to the characteristics of the solution, thus appropriating the modeling process.

References

[1] C.W. van Atta, Stably stratified homogeneous turbulence. A paradigm for geophysical shear flows. International Conference on Turbulent Heat Transfer, San Diego, CA, 10–15 March (1996).

[2] E.C. Itswiere, K.N. Helland, C.W. van Atta, The evolution of grid-generated turbulence in a stably stratified fluid, JFM 162 (1986) 299–338.

[3] E.J. Hopfinger, Turbulence in stratified fluids. A review, J. of Geophysical Research 92 (NC5) (1987) 5287–5303.

[4] T.D. Dickey, G.L. Mellor, Decaying in neutral and stratified fluids, J. of Fluid Mech. 99 (1980) 13–31.

[5] T. Gerz, H. Yamazaki, Direct numerical simulation of buoyancy-driven turbulence in stably stratified fluid, J. of Fluid Mech. 249 (1993) 415–440.

[6] V.A. Kolovandin, V.U. Bondarchuk, C. Meola, G. De Felice, Modeling of the homogeneous turbulence dynamics of stably stratified media, Int. J. of Heat and Mass Transfer 36 (1993) 1953–1968.

[7] J.H. Lienhard, C.W. van Atta, The decay of turbulence in thermally stratified flow, J. of Fluid Mech. 210 (1990) 57–112.

[8] T.P. Sommer, R.W.C. So, J. Zhang, Modeling non-equilibrium and history effects of homogeneous turbulence in a stably stratified medium. International Conference on Turbulent Heat Transfer, San Diego, CA, 10–15 March (1996).

[9] V.A. Babenko, Homogeneous turbulence evolution in stably stratified flow—I. Internal gravity waves at low inverse Froude numbers, Int. J. of Heat and Mass Transfer 40 (1997) 1951–1961.

[10] V.A. Babenko, Homogeneous turbulence evolution in stably stratified flow—II. Asymptotic regimes of large evolution time at low inverse Froude numbers, Int. J. of Heat and Mass Transfer 40 (1997) 1963–1976.

[11] D.W. Dunn, W.H. Reid 1958 Heat transfer in isotropic turbulence during final period of decay. NACA Report. TN4186.

[12] B.A. Kolovandin, Modeling the dynamics of turbulent transport processes, in: Advances in Heat Transfer, vol. 21, Pergamon Press, 1991, pp. 185–234.

[13] A. Nayfeh, Perturbation Methods, Wiley Interscience, New York, 1974.

[14] M. van Dyke, Perturbation Methods in Fluid Mechanics, Academic Press, New York, London, 1964.

[15] Y.G. Lai, R.M.C. So, Near wall modelling of turbulent heat fluxes, Int. J. of Heat and Mass Transfer 33 (1990) 1429–1440.

[16] L. van Haren, C. Staquet, C. Cambon, A study of decaying stratified turbulence by a two-point closure EDQNM model and by direct numerical simulation, in: Proceedings of the 4th International Symposium on Stratified Flows, Grenoble, France, 29 June–2 July, 1994.